Hydrogen recombination due to collisions with He and Ar

Stephen Paolini, Luke Ohlinger, and Robert C. Forrey
Department of Physics, Penn State University, Berks Campus, Reading, Pennsylvania 19610-6009, USA
(Received 10 February 2011; published 27 April 2011)

Quantum-mechanical calculations are reported for hydrogen recombination in the presence of a chemically inert spectator. The calculations employ a square integrable Sturmian basis set to provide a discrete representation of the H_2 continuum. Direct three-body recombination is approximated by computing transitions from the nonresonant continuum. Resonant and nonresonant states are handled on equal footing within the sequential two-step energy transfer mechanism. Theoretical rate coefficients are computed within the equilibrium and steady-state approximations for the density of intermediate molecules. The results are compared with existing experimental data for He and Ar. The sensitivity of the calculations to pressure variations and to changes in the potential energy surface are investigated for He. The reliability of these calculations and their relevance for astrophysical models are discussed.

DOI: 10.1103/PhysRevA.83.042713 PACS number(s): 34.80.Lx, 34.50.−s

I. INTRODUCTION

Atomic and molecular recombination in the presence of a third body, often known as three-body recombination (TBR), is one of the most fundamental types of chemical reactions. Together with the inverse process of collision-induced dissociation (CID), it comprises about half of the reactions that have been identified as important in combustion chemistry [1,2]. Of particular interest is the recombination of hydrogen due to its fundamental importance in astrophysics [3–5] and practical importance in plasma physics and rocket propulsion [6].

The current status for TBR of H_2 due to collisions with H is far from satisfactory. Astrophysical models of primordial star formation [3–5] require TBR rate coefficients as input. A survey of published rate coefficients [7] showed a disagreement by orders of magnitude at the low temperatures that are relevant for H_2 formation in primordial gas. Simulations have shown [5] that this uncertainty fundamentally limits the ability to model the density, temperature, and velocity structure of the gas near the collapsing center of population III stars. TBR of H_2 due to collisions with He and the reverse CID process are also important for many astrophysical environments [8]. Due to the availability of experimental data [9], hydrogen recombination due to He and Ar colliders has provided a convenient testing ground for the development of TBR theories [10,11]. At room temperatures, there is not much difference in the efficiency of these noble gas colliders in catalyzing hydrogen recombination. At lower temperatures, the catalytic efficiency becomes more sensitive to the collider and the calculations more sensitive to the theoretical formulation.

The orbiting resonance theory (ORT) developed by Roberts, Bernstein, and Curtiss [10] has been the most widely used approach for calculating hydrogen recombination rates. The theory assumes a steady-state population of H_2-orbiting resonances and calculates the rate of stabilization due to collisions with a third body. The full set of resonances [12–14] is reduced to a set of six after energy and lifetime considerations are taken into account. Classical trajectories are computed for the restricted set of resonances and the recombination rate constants are determined. Because the ORT mechanism is a sequential process involving two-body collisions, the theory neglects the possibility that the recombination occurs in a single step as a consequence of a direct three-body collision. The influence of three-body collisions was investigated for $H_2 + H_2$ by Schwenke [14,15] and for $Ne_2 + H$ by Pack, Walker, and Kendrick [2,16]. In both cases, the master equations were solved for the kinetics and it was found that three-body collisions were not at all negligible. Similar conclusions were found in other studies (with a detailed historical account provided in Ref. [2]), suggesting that a reexamination of this issue is needed.

Recently, quasiclassical dynamical calculations have been performed [17] which included two-body and three-body collisions in a unified treatment of H_2 recombination due to H. Quantum-mechanical calculations that account for two-body and three-body collisions have also been performed for CID of H_2 due to He [8,18,19]. Advances in present computing power have made it possible to remove many of the approximations that were necessary for earlier calculations. The large internal energy spacing of the H_2 molecule allows quantum-mechanical representations that are sufficiently compact for He and Ar colliders such that numerical convergence is now achievable at low to intermediate collision energies. It should be possible, therefore, to develop a complete set of state-to-state rate coefficients, which may be used in kinetic models to account for both TBR and the inverse process of CID. This goal requires (i) a potential energy surface (PES) that is accurate for all possible coordinate configurations, (ii) a complete set of state-to-state cross sections computed using a fully quantum mechanical formulation, (iii) a coherent inclusion of direct three-body collisions in the dynamics, and (iv) a master equation analysis of the kinetics that includes lifetimes for long-lived resonant states and time delays for short-lived nonresonant states.

In the present work, we address the first three of these requirements. We employ the best available PES for each system and study the sensitivity of our calculations to regions where the PES may be inadequate. We use an L^2 discretization of the continuum that allows for converged dissociation and recombination cross sections. Nonresonant states are handled using the same two-step energy transfer mechanism that is used in ORT to describe resonant states. The quantum-mechanical coupled states (CS) formulation is used to compute the

scattering cross sections. Recombination rate constants are computed using both the equilibrium and steady-state approximations for the population of intermediate molecules. The results for He and Ar are compared to existing experimental data.

II. THEORY

Recombination of H in the presence of an inert third body M may occur through the direct process

$$\mathrm{H} + \mathrm{H} + M \rightarrow \mathrm{H}_2 + M \tag{1}$$

or through the sequential two-step process

$$\mathrm{H} + \mathrm{H} \rightarrow \mathrm{H}_2(u), \tag{2}$$

$$\mathrm{H}_2(u) + M \rightarrow \mathrm{H}_2(b) + M, \tag{3}$$

where b and u designate bound and unbound states. The recombination rate coefficient for the two-step process is given by

$$k_r = \sum_{bu} k_{ub} \frac{[\mathrm{H}_2(u)]}{[\mathrm{H}]^2}, \tag{4}$$

where $[X]$ denotes the density of X, and k_{ub} is the rate coefficient which connects the bound and unbound states. At equilibrium

$$\frac{[\mathrm{H}_2(u)]}{[\mathrm{H}]^2} = \frac{g_u \exp(-E_u/k_B T)}{4 Q_T}, \tag{5}$$

where Q_T is the usual translational partition function and the factor of 4 in the denominator of Eq. (5) is needed to account for the two H atoms approaching each other on the $^1\Sigma_g^+$ electronic state. TBR rate coefficients may be obtained from CID rate coefficients using detailed balance:

$$k_{ub} = \frac{g_b}{g_u} \exp\left(\frac{E_u - E_b}{k_B T}\right) k_{bu}, \tag{6}$$

where g_b and g_u are the degeneracy factors associated with the diatomic energies E_b and E_u. If the unbound states are restricted to quasibound states, then the formulation reduces to the orbiting resonance theory of Roberts, Bernstein, and Curtiss [10]. The three-body continuum contribution may be included in the two-step formulation by allowing nonresonant states in the summation over u in Eq. (4). These nonresonant states represent discretized contributions in a numerical quadrature of the continuum [8]. In this approach, the direct recombination process (1) is treated in the same manner as the contributions from the orbiting resonances. The state-to-state rate coefficient

$$k_{if} = \left(\frac{8 k_B T}{\pi \mu}\right)^{1/2} (k_B T)^{-2} \int_0^\infty \sigma_{if}(E_T) \times \exp(-E_T/k_B T)\, E_T\, dE_T \tag{7}$$

is also extended to include resonant and nonresonant unbound states. In Eq. (7), $E_T = E - E_i$ is the translational energy in the ith channel, μ is the reduced mass of M with respect to H_2, and $\sigma_{if}(E_T)$ is the cross section for the collision.

It is noteworthy that Eq. (4) may be assumed to include lifetime and pressure effects via a steady-state approximation for the formation of the intermediate molecule. The steady-state density is given by

$$\frac{[\mathrm{H}_2(u)]}{[\mathrm{H}]^2} = \frac{k_u^{\mathrm{eq}}}{1 + \tau_u [M] \sum_b k_{ub}}, \tag{8}$$

where τ_u is the lifetime of the unbound diatomic state and k_u^{eq} is the equilibrium constant given in Eq. (5). As noted by Pack, Walker, and Kendrick [16], this steady-state approximation neglects possible repopulation of the intermediate molecules by three-body collisions. Their master equation analysis showed that three-body collisions are essential for keeping the metastable quasibound states from getting depleted at high pressures. Unbound states that are either part of the nonresonant continuum or else correspond to broad above-barrier resonances with negligible lifetimes are unmodified by Eq. (8). These states give rise to pure third-order kinetics for all pressures. The use of Eq. (8) for unbound resonances with significant lifetimes, however, does not give pure third-order kinetics at large pressures due to the neglected $[M]$ dependence in the numerator that arises from three-body collisions [16]. The use of the equilibrium approximation (5), the steady-state approximation (8), and the need for a more detailed master equation analysis for the present system is discussed in the next section.

The collision cross sections are computed quantum mechanically using the coupled states formulation [20,21] for the Hamiltonian

$$H = -\frac{1}{2m} \nabla_r^2 - \frac{1}{2\mu} \nabla_R^2 + V(r, R, \theta), \tag{9}$$

where m is the reduced mass of H_2, r is the distance between the H atoms, R is the distance between M and the center of mass of H_2, and θ is the angle between $\vec{r}$ and $\vec{R}$. The three-dimensional potential energy surface is separated into a diatomic potential $v(r)$ and an interaction potential $V_I(r, R, \theta)$. The diatomic Schrödinger equation

$$\left[\frac{1}{2m}\frac{d^2}{dr^2} - \frac{j(j+1)}{2m\, r^2} - v(r) + \epsilon_{vj}\right] \chi_{vj}(r) = 0 \tag{10}$$

is diagonalized to obtain the eigenstates, $\chi_{vj,}$ for each vibrational and rotational quantum number v and j. The bound and unbound diatomic energies, E_b and E_u, in Eqs. (5)–(7) are determined by the eigenvalues, ϵ_{vj}. The diagonalization is performed by expanding the diatomic eigenstates in an orthonormal Laguerre polynomial $L_n^{(2j+2)}$ basis set

$$\phi_{j,n}(r) = \sqrt{\frac{a n!}{(n + 2j + 2)!}} (ar)^{j+1} \exp(-ar/2) L_n^{(2j+2)}(ar). \tag{11}$$

The full wave function in the body-fixed frame is expanded for a total angular momentum J in the set of diatomic eigenstates as

$$\Psi^{J\Omega}(\vec{R}, \vec{r}) = \frac{1}{R} \sum_{v,j} C_{vj}(R) \chi_{vj}(r) Y_{j\Omega}(\theta, 0), \tag{12}$$

where Ω is the body-fixed projection of both J and j. In the CS formulation, the off-diagonal Coriolis couplings that arise in the body-fixed frame are neglected, and the eigenvalue of

the orbital angular momentum operator $\hat{l}^2$ is approximated by $l(l+1)$, where l is assumed to be a conserved quantum number. This procedure yields the set of coupled equations

$$\left[\frac{d^2}{dR^2} - \frac{l(l+1)}{R^2} + 2\mu(E-\epsilon_{vj})\right] C_{vj}(R) = 2\mu \sum_{v',j'} C_{v'j'}(R)\,\langle vj\Omega|V_I|v'j'\Omega\rangle, \tag{13}$$

where

$$\langle vj\Omega|V_I|v'j'\Omega\rangle = \sum_{\lambda=0}^{\lambda_{\max}} (-1)^{\Omega}[(2j+1)(2j'+1)]^{1/2} \times \begin{pmatrix} j' & \lambda & j \\ 0 & 0 & 0 \end{pmatrix} \begin{pmatrix} j' & \lambda & j \\ \Omega & 0 & -\Omega \end{pmatrix} \langle \chi_{vj}|V_\lambda|\chi_{v'j'}\rangle \tag{14}$$

and V_λ are coefficients for the expansion of the interaction potential in terms of Legendre polynomials P_λ,

$$V_I(r,R,\theta) = \sum_{\lambda=0}^{\lambda_{\max}} V_\lambda(r,R) P_\lambda(\cos\theta). \tag{15}$$

The (...) denotes a 3-j symbol and the matrix element $\langle \chi_{vj}|V_\lambda|\chi_{v'j'}\rangle$ assumes integration over r. The collision cross section is given by

$$\sigma_{vj\to v'j'} = \frac{\pi}{2\mu E_T(2j+1)} \sum_{J=0}^{J_{\max}} (2J+1) \times \sum_{\Omega=0}^{\Omega_{\max}} (2-\delta_{\Omega 0})\left|\delta_{jj'}\delta_{vv'} - S^{J\Omega}_{vj;v'j'}\right|^2, \tag{16}$$

where $S^{J\Omega}_{vj;v'j'}$ is the scattering matrix and $E_T = E - \epsilon_{vj}$. The set of coupled equations (13) may be conveniently solved using the general inelastic scattering program MOLSCAT [22]. The interaction potentials for the two systems are obtained from Refs. [23] and [24]. To describe dissociation and recombination, the PES should provide an accurate representation for all values of H-H separation. For $He + H_2$ [8,25], the dissociation cross sections were found to be insensitive to changes in the Muchnik and Russek (MR) potential for large stretching of the H-H bond ($r > 4$ a.u.). Although the functional form for the dispersion term in the MR potential is not adequate to properly represent the physics [23], the exponential decay contained within the Sturmian representation effectively cuts off the unphysical long-range behavior of the potential. For intermediate stretching ($2 < r < 4$ a.u.), the MR potential is not constrained by *ab initio* data and there is some sensitivity of the cross sections to changes in the parametrization of the potential in this region [25]. This sensitivity is investigated in the next section.

III. RESULTS

Recombination rate coefficients were computed from CID rate coefficients using detailed balance. Cross sections for CID were computed previously for $He + H_2$ for the most weakly bound vibrational levels [8]. We extend these calculations to include more deeply bound vibrational levels and more translational energies near the dissociation thresholds. The same method is then used for computing $Ar + H_2$ cross sections. Rate coefficients are computed from the cross sections using Eq. (7). Figure 1 shows the CID rate coefficients for the two systems when the H_2 molecule is initially in the last bound vibrational level for $j = 0$. The results are very similar, particularly at low temperature. The present results for Ar are also compared with the distorted-wave Born approximation results of Sakai [26]. The comparison shows that the distorted wave results are significantly lower than the present results at low temperatures but agree very well with the present results at high temperatures.

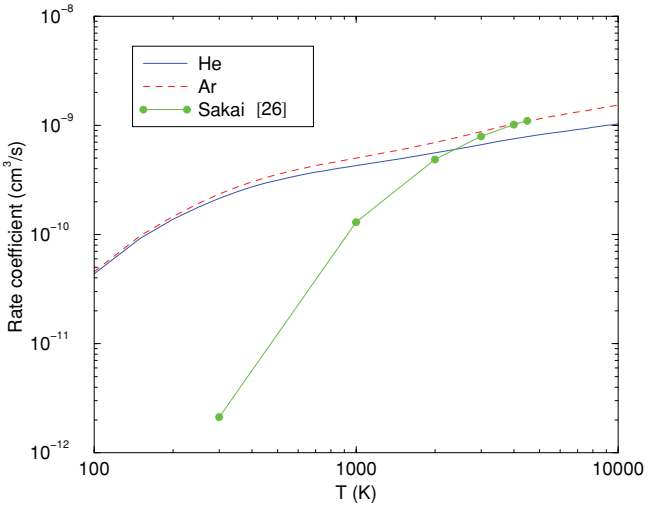

FIG. 1. (Color online) Rate coefficient for CID from $v = 14$, $j = 0$. The solid blue curve (He) and dashed red curve (Ar) are the present results. Also shown for Ar are the distorted-wave Born approximation results of Sakai [26].

Figures 2 and 3 show three-body recombination rate coefficients for $He + H_2$ as a function of temperature. In

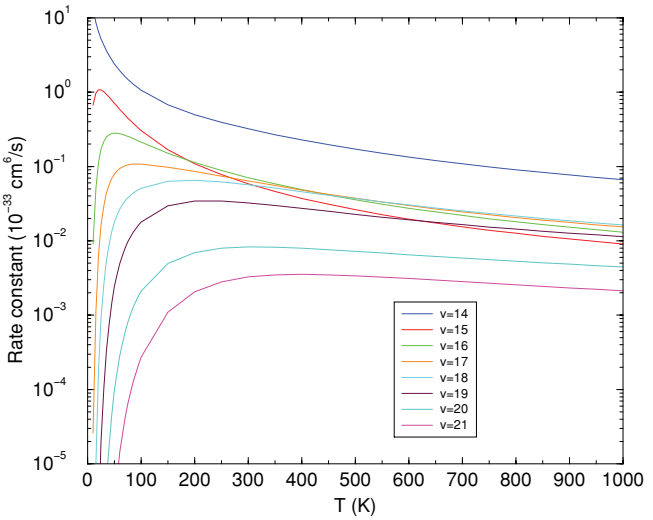

FIG. 2. (Color online) Three-body recombination rate coefficients for $He + H_2$ (v, $j = 4$). The curves show an orderly decrease with v at low temperatures. The $v = 14$ curve corresponds to recombination from a resonant state whereas the $v \geqslant 15$ curves correspond to recombination from positive energy pseudostates.

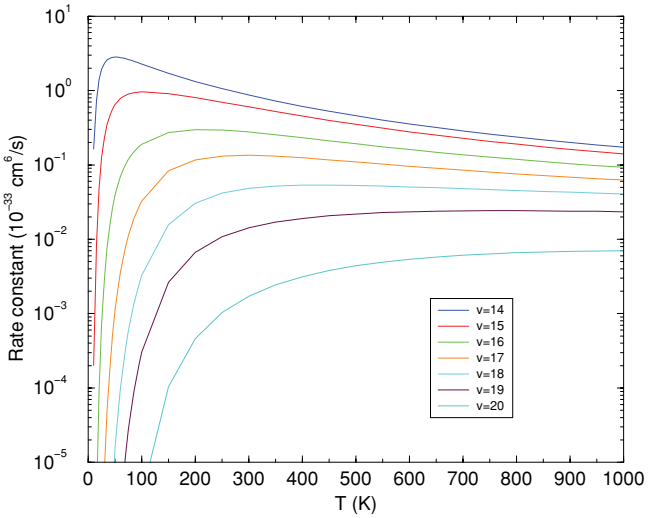

FIG. 3. (Color online) Three-body recombination rate coefficients for $He + H_2$ (v, $j = 5$). The curves show an orderly decrease with v at all temperatures. The $v = 14$ curve corresponds to recombination from a resonant state whereas the $v \geqslant 15$ curves correspond to recombination from positive energy pseudostates.

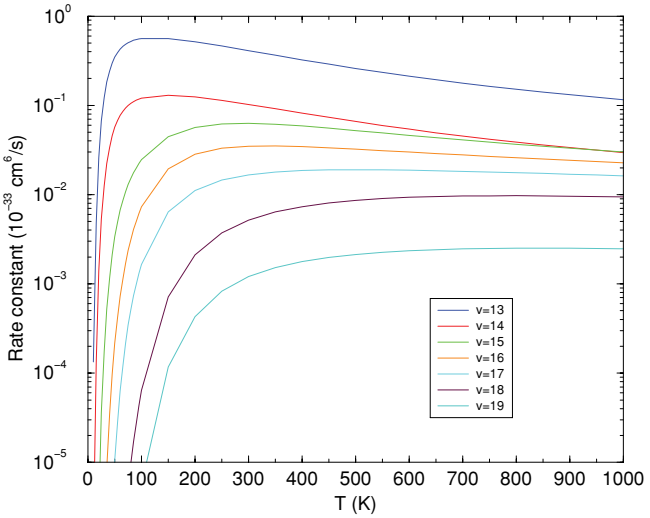

FIG. 4. (Color online) Three-body recombination rate coefficients for $Ar + H_2$ (v, $j = 8$). The curves show an orderly decrease with v at all temperatures. The $v = 13$ curve corresponds to recombination from a resonant state whereas the $v \geqslant 14$ curves correspond to recombination from positive energy pseudostates.

Fig. 2 the curves correspond to recombination from positive energy states of H_2 with $j = 4$. The dominant recombination contribution comes from the $v = 14$ orbiting resonance. This resonance is long-lived with a width of 8.4×10^{-6} cm^{-1} [14]. The remaining $v \geqslant 15$ states are nonresonant. The rate coefficients for these states decrease uniformly with v for low temperature. At higher temperatures, the $v = 15$–19 curves intersect and the recombination rate coefficients are of comparable magnitude. The rate coefficients for $v = 20$ and $v = 21$ are considerably smaller than for $v = 15$–19 for all temperatures, indicating that the basis set is sufficiently converged. In Fig. 3 the curves correspond to recombination from positive energy states of H_2 with $j = 5$. The $v = 14$ state is a resonance state with a width of 15.22 cm^{-1} [14]. Although still the dominant contribution to recombination, the rate coefficient for $v = 14$ is closer in magnitude to that of $v = 15$. The rate coefficients for the nonresonant states, $v = 15$–20, decrease uniformly with v for all temperatures. The contribution from $v = 20$ is significantly smaller than the others, which again indicates that the basis set is sufficiently converged.

Figures 4 and 5 show three-body recombination rate coefficients for $Ar + H_2$ as a function of temperature. Orbiting resonances occur for H_2 ($v = 13$, $j = 8$) and H_2 ($v = 13$, $j = 9$) with widths of 1.485 and 48.28 cm^{-1}, respectively. Figure 4 shows that the resonant contribution for $j = 8$ is clearly dominant over the nonresonant contribution for all temperatures. As in the He case shown in Fig. 3, the rate coefficients for the nonresonant states decrease uniformly with v over the entire temperature range. This is not the case for the $j = 9$ rate coefficients shown in Fig. 5. The $v = 15$ curve crosses the $v = 14$ curve around 400 K and overtakes the resonant $v = 13$ curve around 700 K. Likewise, the $v = 17$ curve crosses the $v = 16$ curve around 300 K and approaches the $v = 14$ curve at 1000 K. The highest energy pseudostate for $j = 9$ corresponds to $v = 18$, which gives a negligible contribution to the total recombination rate and indicates that the basis set is sufficiently converged.

The total resonant and nonresonant three-body recombination rate coefficients for $He + H_2$ are shown in Fig. 6. These results include recombination to either of the two most weakly bound vibrational levels for each rotational level $j \leqslant 20$. Recombinations to more strongly bound levels were found to make a negligible contribution. The resonant and nonresonant contributions were added together to obtain the total rate coefficient that is compared to the experimental data of Trainor *et al.* [9] at 77 and 300 K. The total rate coefficients computed

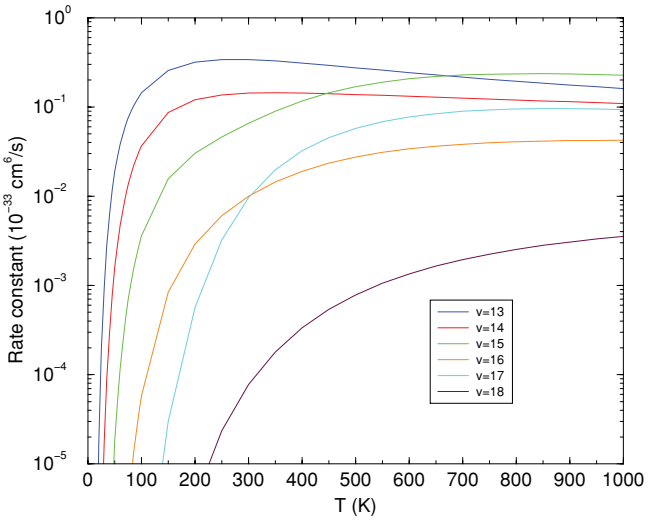

FIG. 5. (Color online) Three-body recombination rate coefficients for $Ar + H_2$ (v, $j = 9$). The curves show an orderly decrease with v at low temperatures. The $v = 13$ curve corresponds to recombination from a resonant state whereas the $v \geqslant 14$ curves correspond to recombination from positive energy pseudostates.

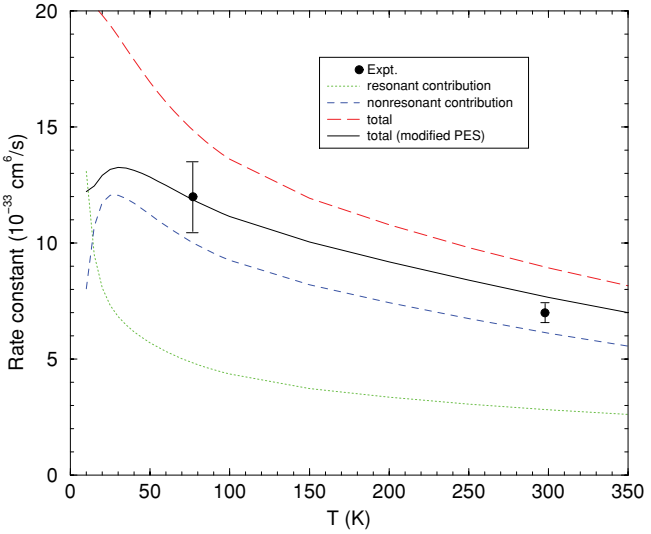

FIG. 6. (Color online) Rate coefficient for three-body recombination of H_2 due to collision with He. The total rate coefficients are obtained as the sum of the resonant and nonresonant contributions. Results for the modified PES (see text) show improved agreement with the experimental data.

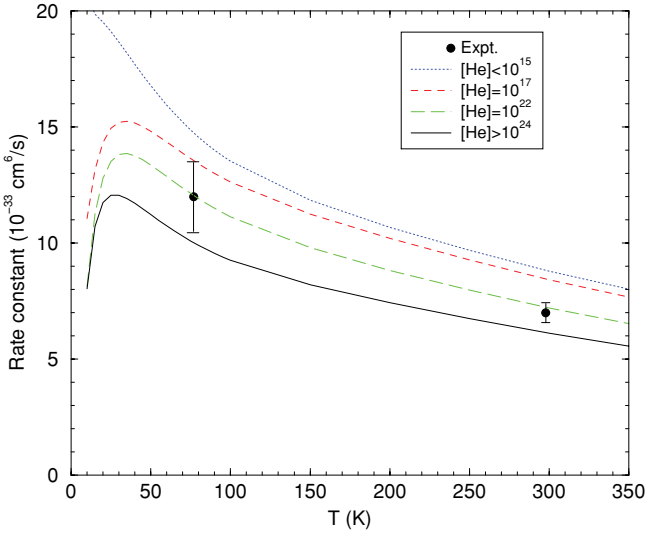

FIG. 7. (Color online) Rate coefficient for three-body recombination of H_2 due to collision with He as a function of density (in units of cm^{-3}). Results for the unmodified PES may be brought into good agreement with the experimental data using Eq. (8) with a density of 10^{22} cm^{-3}.

using the PES of Muchnik and Russek [23] are found to be about 25% larger than the experimental data.

There are several possibilities for this discrepancy. One possibility is the inadequate constraint of the PES for stretching of the H_2 bond beyond 2 a.u. To test this hypothesis, a modified PES was constructed as described in Mack *et al.* [25]. The terms $A_d(r)$ and $\alpha_d(r)$ contained in the original PES [23] were matched to decaying exponential functions of the form Ar exp(−Br). The parameters A and B were determined by the continuity of the functions and their derivatives at $r = 2$ a.u. This modification does not affect the original PES in regions where there is *ab initio* data to constrain the parametrization. For large stretching, the exponential decay contained in the modified PES provides a more realistic r dependence for the terms $A_d(r)$ and $\alpha_d(r)$ than does the linear dependence contained in the original PES [23]. Figure 6 shows that the three-body recombination rate coefficients are in much better agreement with the experimental data when the modified PES is used in the calculations. Of course, the modification described above is not unique and it would be desirable to constrain the $2 < r < 4$ a.u. region with additional *ab initio* data.

Another possibility for the discrepancy between theory and experiment for He is the use of the equilibrium approximation (5). This approximation does not take into account the lifetimes of the intermediate states and may overestimate the resonant contributions at large pressures. The steady-state approximation (8) reduces the resonant contribution and often provides a more accurate estimate of theoretical recombination rate coefficients. Figure 7 illustrates this point using the original MR PES without the modification described above. The theoretical curve decreases with [He] and may be brought into good agreement with the experimental data for [He] = 10^{22} cm^{-3}. The steady-state approximation, while generally more accurate than the equilibrium approximation, still neglects repopulation of intermediate quasibound states due to the three-body collisions. A detailed master equation analysis is needed to fully account for this density dependence. The actual density used in the experiments was not reported, but if it was less than 10^{15} cm^{-3} the steady-state and equilibrium approximations yield essentially the same recombination rate coefficient (see Fig. 7). In this case, a master equation analysis is not needed and the discrepancy between theory and experiment would likely be due to inaccuracies in the PES.

The case of Ar provides a good point of comparison because the He and Ar experiments were performed in a similar manner. The PES for Ar + H_2 [24] was specifically designed for use in energy transfer studies involving dissociation and recombination. The PES provides an accurate account of the H_2 bond length in both the strong bonding and dissociation limits. The recombination rate coefficients computed using this PES, therefore, provide a good test of the reliability of the quantum-mechanical scattering formulation. Figure 8 shows the calculated recombination rate coefficients for Ar + H_2 together with the experimental data of Trainor *et al.* [9]. The comparison shows excellent agreement between theory and experiment at 300 K. There is a large discrepancy, however, between theory and experiment at 77 K. We believe this is due to the neglect in our calculations of the exchange mechanism that produces intermediate states of ArH before recombining to form H_2. This mechanism, which is negligible for He due to its weaker attraction, is expected to become increasingly important for Ar as the temperature is reduced. The agreement at 300 K suggests that the Ar density is probably low enough that the equilibrium approximation is sufficient. The same reasoning further underscores the need to extend the range of *ab initio* data for He + H_2 to the intermediate stretching region ($2 < r < 4$ a.u.).

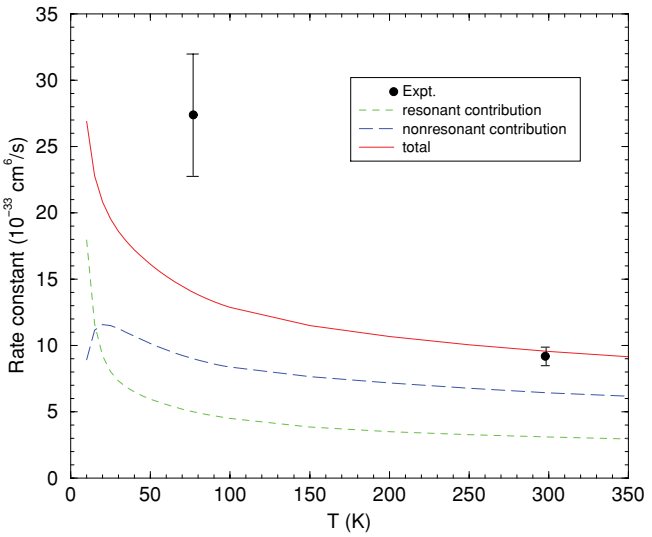

FIG. 8. (Color online) Rate coefficient for three-body recombination of H_2 due to collision with Ar. The total rate coefficients are obtained as the sum of the resonant and nonresonant contributions. The discrepancy at 77 K is likely due to the neglect in our calculations of the exchange mechanism, which produces intermediate states of ArH before recombining to form H_2.

IV. CONCLUSIONS

Rate coefficients for TBR and CID of H_2 due to collisions with He are known to be important for astrophysical models [4,8]. While there are no experimental data available to benchmark the CID calculations, there are existing experimental data available to compare with the TBR calculations. These comparisons show that the present theoretical results are about 25% larger than expected. Two possible reasons for this discrepancy were explored. The PES that was used in the calculations is known to be unconstrained by *ab initio* data for H_2 bonds that are stretched beyond 2 a.u. The TBR and CID calculations were found to be sensitive to this region of the PES. A second possibility was the use of the equilibrium approximation for the population of intermediate molecular states. Good agreement with the experimental data was found at high He density using the steady-state approximation. A third possible reason for the discrepancy between theory and experiment would be the use of the CS formulation that neglects Coriolis couplings in the body-fixed frame. However, based on previous studies, we believe this formulation is adequate at the temperatures considered in the present case. The agreement between theory and experiment found here for TBR due to Ar collisions at 300 K also attests to the reliability of the CS formulation. The Ar results suggest that the equilibrium approximation is probably adequate for the conditions of the experiment. Therefore, we conclude that the largest source of theoretical uncertainty for He comes from the unconstrained region of the MR PES. Considering the success of this PES for calculating elastic and inelastic processes [27] over a large range of energies, it would be desirable to extend the surface by adding *ab initio* data in the unconstrained region ($2 < r < 4$ a.u.) and recompute the TBR rate coefficients.

Although a 25% discrepancy between theory and experiment is not ideal, it is unlikely to make a significant difference in astrophysical models even if all the error is on the theoretical side. However, the current status for TBR of H_2 due to collisions with H is considerably worse than for He. One of the motivations of this work was to develop a theory of TBR which includes important nonresonant processes and is fully quantum mechanical. This goal has been met for the case of chemically inert spectators. The next issue that must be faced is how to extend the theory to include exchange mechanisms. In addition to the important astrophysical $H + H_2$ TBR system, it has recently been shown that a wide variety of cold trappable van der Waals molecules can be produced via TBR in a buffer gas loaded magnetic trap [28,29]. Theoretical support for these low-temperature experiments requires a fully quantum mechanical description that includes exchange mechanisms. It is hoped that some of the theoretical methods developed in this work may be useful in addressing recombination for these important systems.

ACKNOWLEDGMENTS

This work was supported by NSF Grant No. PHY-0854838. Helpful conversations with N. Balakrishnan, P. C. Stancil, T. Tscherbul, and H. R. Sadeghpour are gratefully acknowledged.

[1] D. L. Baulch *et al.*, J. Phys. Chem. Ref. Data **21**, 411 (1992).
[2] R. T. Pack, R. B. Walker, and B. K. Kendrick, J. Chem. Phys. **109**, 6701 (1998).
[3] D. R. Flower and G. J. Harris, Mon. Not. R. Astron. Soc. **377**, 705 (2007).
[4] S. C. O. Glover and T. Abel, Mon. Not. R. Astron. Soc. **388**, 1627 (2008).
[5] M. J. Turk, P. Clark, S. C. O. Glover, T. H. Greif, T. Abel, R. Klessen, and V. Bromm, Astrophys. J. **726**, 55 (2011).
[6] A. E. Orel, J. Chem. Phys. **87**, 314 (1987).
[7] S. Glover, in *American Institute of Physics Conference Series, Santa Fe, 2007*, edited by B. W. O'Shea, A. Heger, and T. Abel, Vol. 990 (American Institute of Physics, Melville, NY, 2007), p. 25.
[8] L. Ohlinger, R. C. Forrey, T.-G. Lee, and P. C. Stancil, Phys. Rev. A **76**, 042712 (2007).
[9] D. W. Trainor, D. O. Ham, and F. Kauffman, J. Chem. Phys. **58**, 4599 (1973).
[10] R. E. Roberts, R. B. Bernstein, and C. F. Curtiss, J. Chem. Phys. **50**, 5163 (1969).
[11] P. A. Whitlock, J. T. Muckerman, and R. E. Roberts, J. Chem. Phys. **60**, 3658 (1974).
[12] T. G. Waech and R. B. Bernstein, J. Chem. Phys. **46**, 4905 (1967).
[13] R. J. LeRoy and R. B. Bernstein, J. Chem. Phys. **54**, 5114 (1971).
[14] D. W. Schwenke, Theor. Chim. Acta **74**, 381 (1988).
[15] D. W. Schwenke, J. Chem. Phys. **92**, 7267 (1990).
[16] R. T. Pack, R. B. Walker, and B. K. Kendrick, J. Chem. Phys. **109**, 6714 (1998).

[17] F. Esposito and M. Capitelli, J. Phys. Chem. A **113**, 15307 (2009).
[18] K. Sakimoto, Chem. Phys. **236**, 123 (1998); J. Chem. Phys. **110**, 11233 (1999); Chem. Phys. **249**, 1 (1999); J. Chem. Phys. **112**, 5044 (2000).
[19] T. Takayanagi and A. Wada, Chem. Phys. **277**, 313 (2002).
[20] R. T. Pack, J. Chem. Phys. **60**, 633 (1974).
[21] P. McGuire and D. J. Kouri, J. Chem. Phys. **60**, 2488 (1974); P. McGuire, *ibid.* **62**, 525 (1975).
[22] J. M. Hutson and S. Green, MOLSCAT computer code, version 14 (1994), distributed by Collaborative Computational Project No. 6 of the Engineering and Physical Sciences Research Council (UK).
[23] P. Muchnick and A. Russek, J. Chem. Phys. **100**, 4336 (1994).
[24] D. W. Schwenke, S. P. Walch, and P. R. Taylor, J. Chem. Phys. **98**, 4738 (1993).
[25] A. Mack, T. K. Clark, R. C. Forrey, N. Balakrishnan, T.-G. Lee, and P. C. Stancil, Phys. Rev. A **74**, 052718 (2006).
[26] K. Sakai, Chem. Phys. **220**, 115 (1997).
[27] T.-G. Lee, C. Rochow, R. Martin, T. K. Clark, R. C. Forrey, N. Balakrishnan, P. C. Stancil, D. R. Schultz, A. Dalgarno, and G. J. Ferland, J. Chem. Phys. **122**, 024307 (2005).
[28] N. Brahms, B. Newman, C. Johnson, T. Greytak, D. Kleppner, and J. Doyle, Phys. Rev. Lett. **101**, 103002 (2008).
[29] N. Brahms, T. V. Tscherbul, P. Zhang, J. Klos, H. R. Sadeghpour, A. Dalgarno, J. M. Doyle, and T. G. Walker, Phys. Rev. Lett. **105**, 033001 (2010).